Chem Biol Drug Des 2015; **86:** 447–458

Research Article

Synthesis and Structure–Activity Relationships of Triazaspirodecanone Derivatives as Nociceptin/Orphanin FQ Receptor Ligands

Sandra Corrado[1], Umberto M. Battisti[1], Claudia Sorbi[1], Annalisa Tait[1], Davide Malfacini[2], Valeria Camarda[2], Girolamo Calò[2] and Livio Brasili[1,*]

[1]Department of Life Sciences, University of Modena & Reggio Emilia, Via G. Campi 183, 41125 Modena, Italy
[2]Department of Medical Sciences, Section of Pharmacology and National Institute of Neuroscience, University of Ferrara, 44121 Ferrara, Italy
**Corresponding author: Livio Brasili, livio.brasili@unimore.it*

Several spiroxatrine derivatives were synthesized and evaluated as potential NOP receptor ligands. Structural modifications of the 1,4-benzodioxane moiety of spiroxatrine have been the focus of this research project. The structure–activity relationships that emerged indicate that the presence of an *H-bond donor group* (hydroxyl group) is more favorable for NOP activity when it is positioned α with respect to the CH_2 linked to the 1-phenyl-1,3,8-triaza-spiro[4.5]decan-4-one portion. Moreover, *cis* diastereoisomers of the *hydroxyl derivatives* 4 and 22 show a moderately higher degree of stereoselectivity than trans isomers. In particular, the spiropiperidine derivative *cis*-4 has submicromolar agonistic activity, and it will be the reference compound for the design and synthesis of new NOP agonists.

Key words: agonists, NOP ligands, ORL-1, spiroxatrine, triazaspirodecanone

Received 17 July 2014, revised 17 October 2014 and accepted for publication 15 December 2014

The superfamily of G protein-coupled receptors (GPCRs) still represents the majority of current drug targets. Beside the three classical opioid receptors, namely μ,δ and κ, a new rhodopsin-type GPCR, belonging to the opioid family, has been discovered in 1994 and named opioid receptor-like 1 (ORL-1) (1,2). The similarity of postreceptor transduction and the high degree of structural homology (~60%) with the classical opioid receptors suggested that this receptor could be involved in pain modulation (3,4). Moreover, due to its wide distribution, it has been suggested that the ORL-1 receptor may play an important role in many other central nervous system (CNS) processes and in several biological functions such as learning and memory, attention, emotions, homeostasis, neuroendocrine secretions, anxiety, drug abuse, cardiovascular control, immunity, and motor activity (5–11). The endogenous ligand of ORL-1 receptor is a 17-amino acid neuropeptide which was isolated from the brain and named nociceptin/orphanin FQ (N/OFQ) (1,2). The ORL-1 receptor was then renamed nociceptin/orphanin FQ peptide (NOP) receptor. The endogenous peptide ligand inhibits synaptic transmission in the CNS and thereby contributes to a reduction in responsiveness to stress and evokes anxiolytic effects (12). Therefore, NOP selective ligands may represent a novel therapeutic approach for the treatment of neuronal dysfunction, anxiety, and several other CNS pathologies (13). In addition, NOP ligands may be new promising tools for the treatment of acute and chronic pain, possibly by generating drugs with a lower side-effect profile (3–5). In the last decade, several classes of NOP agonists have been reported; they can be divided into peptide and non-peptide ligands. Different chemical classes of non-peptide ligands have been discovered; among them, spiropiperidine analogues have shown relatively higher NOP-binding affinities (14). Spiroxatrine (**1**, Figure 1), an α_2 adrenergic and 5-HT_{1A} antagonist, due to its good affinity for NOP receptor, has been extensively studied to develop ORL-1 selective ligands (15,16). These studies led to the development of the most extensively studied agonist Ro 64-6198 and to other several triazaspirodecanone derivatives (17–19).

Herein, SAR studies on triazaspirodecanone derivatives as potential NOP agonists are reported. In particular, we explored possible substitution of the lipophilic moiety attached to the piperidine nitrogen by a '1-carbon' linker. This kind of studies could represent a useful tool for the development of agonists as the presence of a 1-carbon linker could influence the intrinsic activity of NOP receptor (19). These investigations were focused on the structural variations of the 1,4-benzodioxane moiety of spiroxatrine.

Methods and Materials

Chemistry

All reagents, solvents, and other chemicals were used as purchased from Sigma-Aldrich without further purification

 doi: 10.1111/cbdd.12505

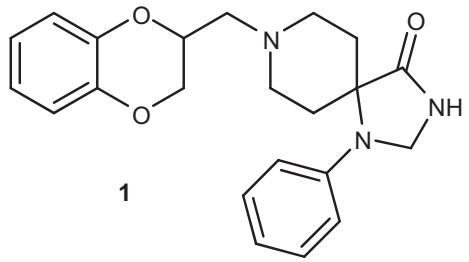

1

Figure 1: Spiroxatrine (**1**).

unless otherwise specified. Air- or moisture-sensitive reactants and solvents were employed in reactions carried out under nitrogen atmosphere unless otherwise noted. Flash column chromatography purifications (medium pressure liquid chromatography) were carried out using Merck silica gel 60 (230–400 mesh; ASTM). The purity of compounds was determined by elemental analysis (C, H, N) that was performed on a Carlo Erba 1106 Analyzer in the Microanalysis Laboratory of the Life Sciences Department of *Università degli Studi di Modena e Reggio Emilia*. Melting points were determined with a Stuart SMP3, and they are uncorrected. The structures of all isolated compounds were established by nuclear magnetic resonance (NMR) and mass spectrometry. ^{1}H and ^{13}C NMR (1D and 2D experiments) spectra were recorded on a DPX-200 Avance (Bruker, Faellanden, Switzerland) spectrometer at 200 MHz (^{1}H-NMR) and on a DPX-400 Avance (Bruker) spectrometer at 400 MHz (^{1}H-NMR) and 100 MHz (^{13}C NMR). Chemical shifts are expressed in δ (ppm). ^{1}H NMR chemical shifts are relative to tetramethylsilane (TMS) as internal standard. ^{13}C NMR chemical shifts are relative to TMS at δ 0.0 or to the ^{13}C signal of the solvent: $CDCl_3$ δ 77.04, CD_3OD δ 49.8, DMSO-d_6 δ 39.5. ^{1}H NMR data are reported as follows: chemical shift, multiplicity (s, singlet; d, doublet; t, triplet; q, quartet; m, multiplet; and br, broadened), number of protons, coupling constants (Hz) and assignment (chr = chromane, chroman-4-one, chroman-4-ol, chromene, chromen-4-one; Ph = phenyl; ox. ac. = oxalic acid; tasd = 1-phenyl-1,3,8-triaza-spiro[4.5]decan-4-one; tetr = tetralone, tetralinol; thn = tetrahydronaphthalene; and Ts = tosyl). ^{1}H-^{1}H correlation spectroscopy (COSY), ^{1}H-^{13}C heteronuclear single-quantum coherence (HSQC) and heteronuclear multiple-bond connectivity (HMBC) NMR 2D experiments were recorded for determination of ^{1}H-^{1}H and ^{1}H-^{13}C correlations, respectively. Mass spectra were obtained on a hybrid Q-TOF mass spectrometer (PE SCIEX-QSTAR) using electrospray ionization mode (HRMS (ESI), ion voltage of 4800 V). The HPLC experimental conditions of the HPLC–MS system were as follows: flow rate 5 mL/min, sample solution (100–1000 pmol/mL) of the selected compound with 0.1% acetic acid, mobile phase consisting of methanol (50%) and water (50%). All compounds were synthesized as reported in Schemes 1–5. Full characterization as well as detailed experimental procedures for all compounds is reported in Appendix S1. The oxalate salts of all tested compounds were used for the pharmacological evaluations.

Biology

N/OFQ and dermorphin used in this study were prepared and purified as previously described (20,21). All cell culture media and supplements were from Invitrogen (Paisley, UK). Dynorphin A, DPDPE, and J-113397 were from Tocris Bioscience (Bristol, UK), while other reagents were from Sigma Chemical Co. (Poole, UK) or E. Merck (Darmstadt, Germany) and were of the highest purity available. N/OFQ, dermorphin, dynorphin A, and DPDPE were solubilized in bidistilled water at a final concentration of 1 mM. All the tested compounds were solubilized in dimethyl sulfoxide at a final concentration of 10 mM. Stock solutions of ligands were stored at −20 °C. The successive dilutions were made in HBSS/HEPES (20 mM) buffer (containing 0.005% BSA fraction V).

Calcium mobilization assay

Chinese hamster ovary (CHO) cells stably co-expressing human recombinant NOP, MOP, or KOP receptors and the C-terminally modified $G\alpha_{qi5}$ and CHO cells stably co-expressing the human recombinant DOP receptor and the $G\alpha_{qG66Di5}$ chimeric protein were generated as previously described (22).

The cells were cultured in culture medium consisting of Dulbecco's MEM/HAMS F12 (50/50) supplemented with 10% fetal calf serum, penicillin (100 IU/mL), streptomycin (100 mg/mL), geneticin (G418; 200 μg/mL), and hygromycin B (100 μg/mL). Cell cultures were kept at 37 °C in 5% CO_2/humidified air. When confluence was reached (3–4 days), cells were subcultured as required using trypsin/EDTA and used for experimentation. Cells were seeded at a density of 50 000 cells/well into 96-well black, clear-bottom plates. After 24-h incubation, the cells were loaded with medium supplemented with 2.5 mM probenecid, 3 μM of the calcium-sensitive fluorescent dye Fluo-4 AM, and 0.01% pluronic acid, for 30 min at 37 °C. Afterward, the loading solution was aspirated, and 100 μL/well of assay buffer: Hank's balanced salt solution (HBSS) supplemented with 20 mM HEPES, 2.5 mM probenecid, and 500 μM brilliant black was added. After placing both plates (cell culture and compound plate) into the FlexStation II, fluorescence changes were measured.

Data analysis and terminology

All data are expressed as means ± standard error of the mean (SEM) of at least three experiments performed in duplicate. For potency values, 95% confidence limits were indicated. Calcium mobilization data are expressed as fluorescence intensity units (FIU) in percent over the baseline. Agonist potencies are given as pEC_{50} corresponding to the negative logarithm of the concentration of the agonist that produces 50% of the maximal effect. Concentration–response curve to agonists was fitted with the following equation:

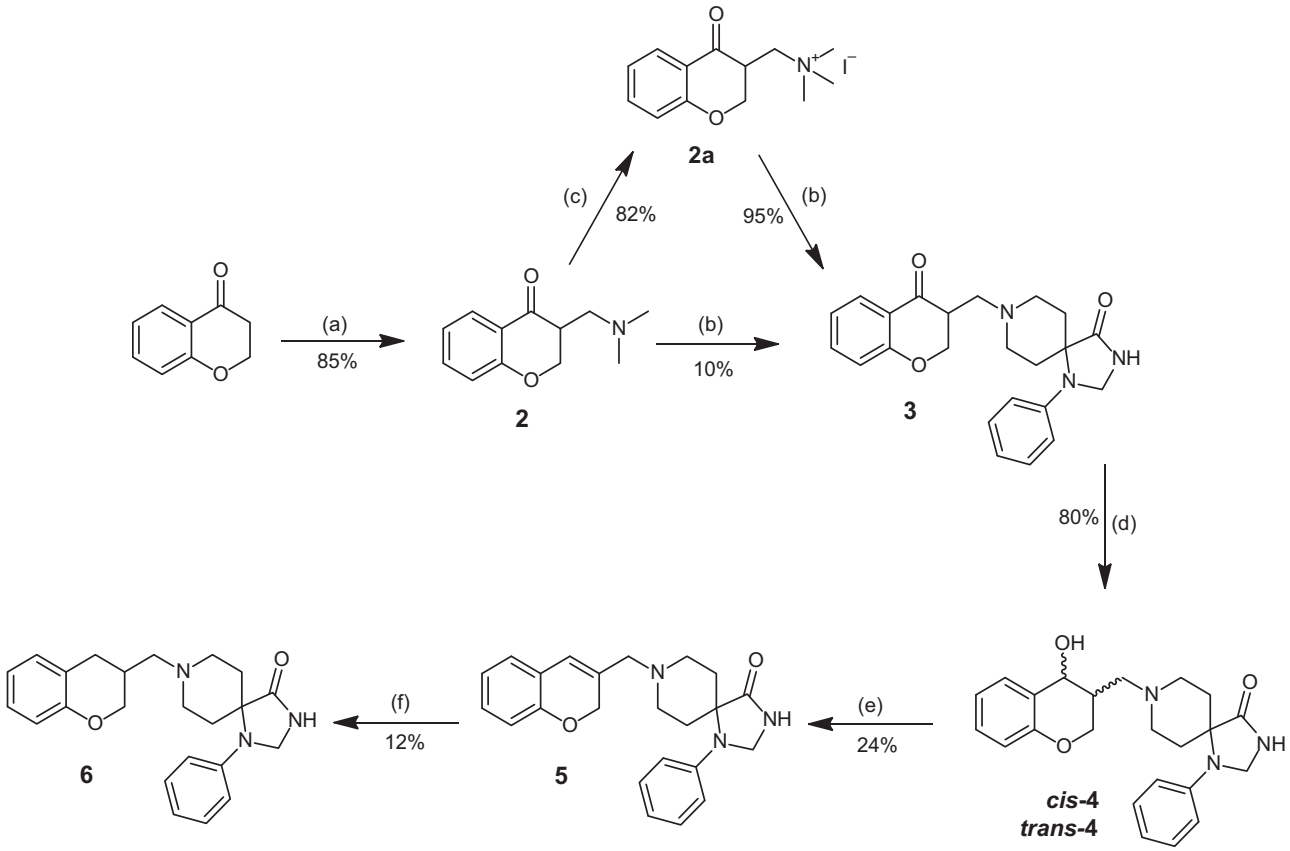

Scheme 1: Synthesis of **3** and its derivatives **4**, **5** and **6**. Reagents and conditions: (a) $(HCHO)_n$, $NH(CH_3)_2{\cdot}HCl$, HCl, EtOH, reflux; (b) 1-phenyl-1,3,8-triaza-spiro[4.5]decan-4-one, Na_2CO_3, acetonitrile, reflux; (c) CH_3I, diethyl ether, 0 °C to r.t.; (d) $NaBH_4$, MeOH, 0 °C to r.t.; (e) H_3PO_4, 60 °C; (f) H_2, Pd/C, MeOH, r.t.

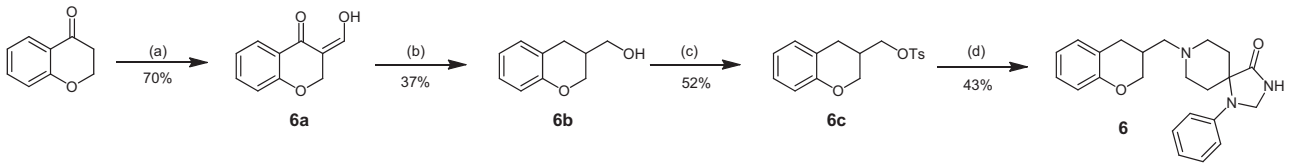

Scheme 2: Alternative synthesis of **6**. Reagents and conditions: (a) $HCOOC_2H_5$, NaO*t*Bu, diethyl ether, 0 °C to r.t.; (b) $BF_3{\cdot}$etherate, $BH_3{\cdot}N(t\text{-}Bu)_3$, CH_2Cl_2, −78 °C to r.t.; (c) TsCl, $N(Et)_3$, CH_2Cl_2, 0 °C to r.t.; (d) 1-phenyl-1,3,8-triaza-spiro[4.5]decan-4-one, Na_2CO_3, acetonitrile, reflux.

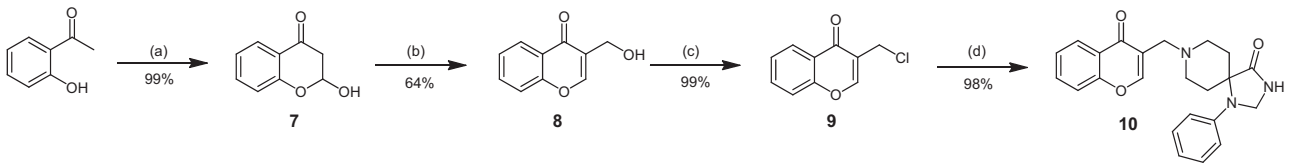

Scheme 3: Synthesis of **10**. Reagents and conditions: (a) $HCOOC_2H_5$, NaOMe, THF, 0 °C to r.t.; (b) CH_2O 37%, NaOAc, HCl, acetone, r.t.; (c) $SOCl_2$, CH_2Cl_2, 0 °C to r.t.; (d) 1-phenyl-1,3,8-triaza-spiro[4.5]decan-4-one, K_2CO_3, KI, acetonitrile, reflux.

$$\text{Effect} = \text{baseline} + \frac{E_{max} - \text{baseline}}{1 + 10^{(\log EC_{50} - X)\cdot n}}$$

where X is the agonist concentration and n is the Hill coefficient.

Agonist efficacy is expressed as intrinsic activity (α) using the maximal effect elicited by N/OFQ as internal standard (α = 1.00).

Antagonist potencies are given as pK_B values. These were derived from inhibition–response curves and calculated,

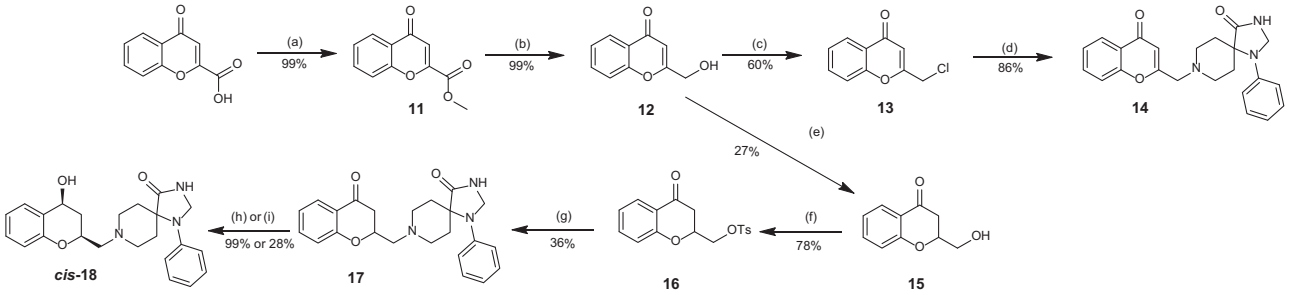

Scheme 4: Synthesis of **14**, **17** and ***cis*-18**. Reagents and conditions: (a) MeOH, H_2SO_4, reflux; (b) $NaBH_4$, MeOH, 0 °C to r.t.; (c) $SOCl_2$, CH_2Cl_2, 0 °C to r.t.; (d) 1-phenyl-1,3,8-triaza-spiro[4.5]decan-4-one, K_2CO_3, KI, acetonitrile, reflux; (e) H_2, Pd/C, CH_2Cl_2, r.t.; (f) TsCl, $N(Et)_3$, CH_2Cl_2, 0 °C to r.t.; (g) 1-phenyl-1,3,8-triaza-spiro[4.5]decan-4-one, Na_2CO_3, acetonitrile, reflux; (h) $NaBH_4$, MeOH, 0 °C to r.t.; (i) L-Selectride, THF, −78 °C to r.t.

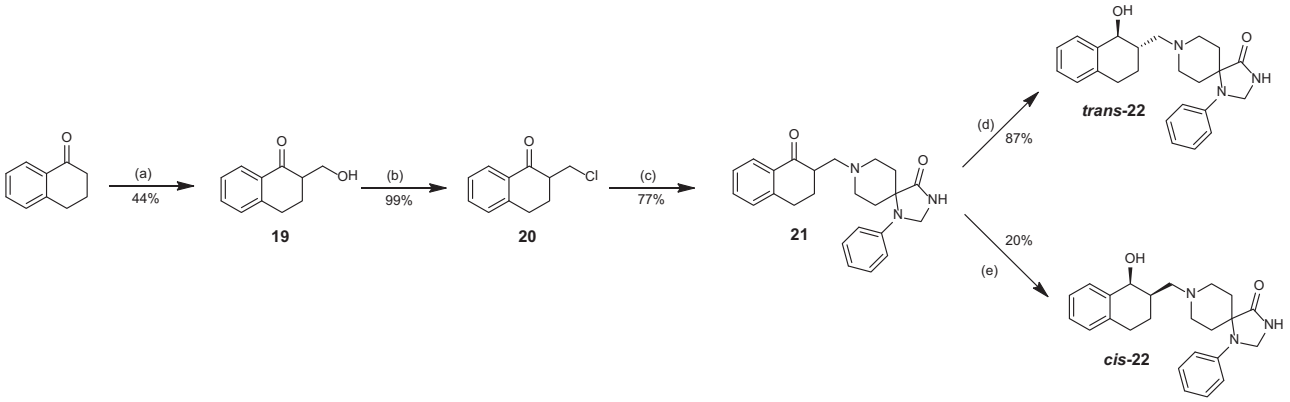

Scheme 5: Synthesis of ***trans*-22** and ***cis*-22**. Reagents and conditions: (a) HCHO 37%, Na_2CO_3, acetonitrile, 40 °C (b) $SOCl_2$, CH_2Cl_2, 0 °C to r.t.; (c) 1-phenyl-1,3,8-triaza-spiro[4.5]decan-4-one, K_2CO_3, KI, acetonitrile, reflux; (d) $NaBH_4$, MeOH, r.t.; (e) L-Selectride, THF, −78 °C to r.t.

assuming a competitive type of antagonism, using the following equation:

$$pK_B = -\log \frac{IC_{50}}{\left(\left[2 + \left(\frac{[A]}{EC_{50}}\right)^n\right]^{1/n}\right) - 1}$$

where IC_{50} is the concentration of antagonist that produces 50% inhibition of the agonist response, [A] is the concentration of agonist, EC_{50} is the concentration of agonist that produces a 50% of the maximal response, and n is the Hill coefficient of the concentration–response curve to the agonist.

Results and Discussion

Synthesis

Synthesis of 8-(4-oxo-chroman-3-ylmethyl)-1-phenyl-1,3,8-triaza-spiro[4.5]decan-4-one (**3**) and its derivatives is outlined in Scheme 1. Compound **2** was prepared by Mannich reaction from dimethylamine hydrochloride and chroman-4-one. Then, the dimethylamino portion of **2** was substituted with the commercially available 1-phenyl-1,3,8-triaza-spiro[4.5]decan-4-one to provide compound **3** (23). Under these conditions, **3** was obtained in poor yield (10% yield). Accordingly, **2** was converted into the corresponding trimethylammonium salt **2a** to increase the efficiency of the leaving group and to enhance the yield of the subsequent substitution reaction (78% yield two steps). From compound **3,** several derivatives were then synthesized. The reduction of the ketone carbonyl group by $NaBH_4$ gave **4** (23) in good yield as *cis/trans* diastereoisomeric mixture (40/60 *cis/trans* ratio). The two diastereoisomers were separated by flash chromatography. The *cis/trans* configuration, relative to 1-phenyl-1,3,8-triaza-spiro[4.5] decan-4-one and OH substituents respectively on 3 and 4 position of chromane ring, was unambiguously assigned through NMR 2D experiments. Positive NOE effect was detected between H-3 and H-4 of the chromane moiety of *cis* isomer (Figure 2). The same signal was not observed in the same NMR 2D experiment performed on *trans* isomer. Stereochemical assignments were confirmed also by the ^{1}H-NMR correlations. The relative chemical shifts of the H-4 protons were particularly informative, as were the H-3-H-4 coupling constants. H-4 signal of the *trans*

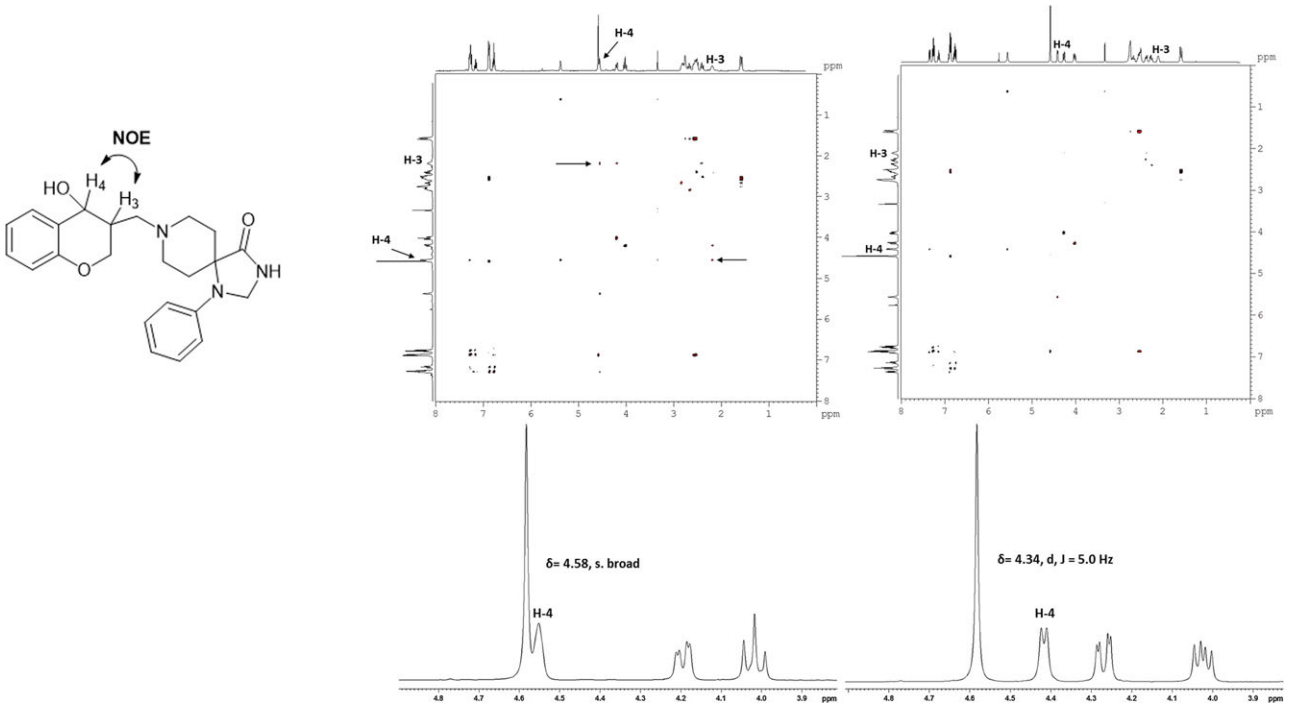

Figure 2: Upper panels: NOESY spectra (DMSO, 400 MHz) of ***cis*-4** (left) and ***trans*-4** (right). Lower panels: enlarged ^{1}H-NMR spectra (DMSO, 400 MHz) of ***cis*-4** (left) and ***trans*-4** (right): 3.9–4.8 ppm region.

isomer occurred at higher field with respect to the H-4 signal of the *cis* isomer (Δδ: 0.28 ppm; Figure 2). The increased deshielding effect produced by the aromatic ring of chromane indicated an equatorial orientation of H-4 proton. Moreover, the H-4 signal of the *cis* isomer appeared as broadened single peak. This small magnitude coupling constant clearly indicated an axial orientation of the H-3 (Figure 2), and these equatorial/axial positions can be observed only in a *cis* configuration. Spectrum of the *trans* isomer showed the H-4 proton as a doublet (J = 5.0 Hz) confirming the axial orientation of both H-3 and H-4 of the chromane ring and thus the *trans* configuration.

Subsequently, compound **5** was obtained by dehydration of chroman-4-ol portion of **4**, in acidic medium. To avoid product degradation due to the harsh conditions of this type of reaction, phosphoric acid was employed. Then, compound **6** was produced by catalytic reduction (Pd/C) of double bond of the chromene moiety of **5**. As we isolated **6** with poor yield (12% yield), we developed a different synthesis which is described in Scheme 2 (23,24). Chroman-4-one was treated in basic conditions with ethyl formate to give **6a** (24). This intermediate was then reduced by the synergistic action of boron trifluoride diethyl etherate and borane *tert*-butylamine complex giving the second intermediate **6b** (25). The latter was then converted into the corresponding tosylated product **6c**, which was then reacted with 1-phenyl-1,3,8-triaza-spiro [4.5]decan-4-one to give **6**.

Furthermore, 8-(4-oxo-4*H*-chromen-3-ylmethyl)-1-phenyl-1,3,8-triaza-spiro[4.5]decan-4-one (**10**), the 2,3-dehydro analogue of **3**, was synthesized as displayed in Scheme 3. Compound **7** (2-hydroxy-chroman-4-one) was obtained by Claisen condensation of 2′-hydroxyacetophenone with ethyl formate. Treatment of **7** with formaldehyde provided the corresponding unstable 3-hydroxymethyl derivative, which was then dehydrated *in situ* to give 3-(hydroxymethyl)-4*H*-chromen-4-one (**8**) (26). Compound **8** was then converted into 3-chloromethyl intermediate **9**, using $SOCl_2$, which was subsequently employed to alkylate 1-phenyl-1,3,8-triaza-spiro[4.5]decan-4-one providing the final compound **10**.

Moreover, the 1-phenyl-1,3,8-triaza-spiro[4.5]decan-4-one portion was inserted at position 2 of the chromane nucleus (Scheme 4). The 4-oxo-4*H*-chromene-2-carboxylic acid was converted into the corresponding methyl ester **11**, and the latter was reduced with $NaBH_4$ to give 2-(hydroxymethyl)-4*H*-chromen-4-one (**12**) (27,28). Compound **12** reacted with $SOCl_2$ to give the chloro-intermediate **13** which furnished **14** in good yields by nucleophilic substitution, under basic conditions, with 1-phenyl-1,3,8-triaza-spiro[4.5]decan-4-one. On the other hand, the reduction of the intermediate **12** provided the 2,3-dihydro derivative **15**, which was subsequently tosylated (**16**) and then reacted with 1-phenyl-1,3,8-triaza-spiro[4.5]decan-4-one to give final compound **17**. The reduction of the latter with $NaBH_4$ or L-Selectride yielded in both cases the 4-hydroxy-chromane derivative **18** exclusively as *cis* isomer

(configuration assignment was performed as previously described for **4**).

For the preparation of the other 1-phenyl-1,3,8-triaza-spiro[4.5]decan-4-one analogues, containing the tetralin nucleus, the same synthetic pathway shown in Scheme 1 was initially followed (5–10% yield). However, to obtain these derivatives in superior yields, we developed a new synthetic strategy (Scheme 5), as the Mannich reaction was proved to be the bottleneck of the previous one, probably due to the instability of the first intermediate. The hydroxymethylation of tetralone in the α position with respect to the carbonyl function was obtained (**19**) using aqueous formaldehyde with base catalysis (29). Subsequently, the corresponding halide **20** was generated by treating the alcohol with $SOCl_2$. Then, alkylation of 1-phenyl-1,3,8-triaza-spiro[4.5]decan-4-one furnished compound **21** (34% yield three steps). Stereoselective reduction of the latter with $NaBH_4$ or L-Selectride gave respectively ***trans*-22** and ***cis*-22** diastereoisomers in good yields (configuration assignment was performed as previously described for **4**) (23). Differently, compound **23** was synthesized starting from α-tetralone as described for compound **6** and as depicted in Scheme 2.

Table 1: ^{1}H and ^{13}C NMR data in $CDCl_3$[a] for compound **3**

Substructures of compound 3	Position[b]	δ ^{1}H (multiplicity, J in Hz)[c]	δ ^{13}C[c]
tasd[d]	2	4.79 (s)	59.2
	3	7.73 (br s)	–
	4	–	178.4
	5	–	59.5
	6/10	1.77 (m), 2.85 (m)[e]	29.1, 29.4
	7/9	2.85 (m)[e]	51.3, 54.4
	1′	–	143.2
	2′/6′	6.94 (d, 8.0)	115.2
	3′/5′	7.34 (dd, 7.5, 8.3)	129.32
	4′	6.91 (t, 7.5)	118.9
chroman-4-one	2″	4.53 (dd, 8.3, 11.4), 4.71 (dd, 4.2, 11.3)	69.7
	3″	2.85 (m)[e]	44.4
	4″	–	193.8
	4″a	–	161.7
	5″	7.94 (dd, 1.7, 7.9)	127.34
	6″	7.07 (dd, 7.1, 7.9)	121.4
	7″	7.52 (ddd, 1.7, 7.1, 8.3)	135.9
	8″	7.03 (d, 8.3)	117.8
	8″a		120.9
	Z	2.85 (m)[e]	48.9

[a]See Methods and Materials.
[b]Atom position in the respective portion of 3.
[c]Measured at 400 MHz.
[d]tasd: 1-phenyl-1,3,8-triaza-spiro[4.5]decan-4-one.
[e]Overlapped with each other.

Purity of the final products

Full assignments of protons and carbons for all the final 1-phenyl-1,3,8-triaza-spiro[4.5]decan-4-one derivatives were performed by ^{1}H and ^{13}C NMR analysis, through related 1D spectra acquisition. Also the evaluation of the key cross-peaks detected in the ^{1}H-^{1}H COSY, ^{1}H-^{13}C HSQC and HMBC 2D NMR experiments was performed. Particularly, the NMR ^{1}H and ^{13}C assignments of compound **3** are reported in Table 1. All the tested compounds were converted into their oxalate salts using oxalic acid in acetone or methanol. The purities of all salts were checked by elemental analysis. The exact mass of all of them was obtained with HPLC–QTOF analysis.

In vitro *biological activity at NOP receptors*

The activities at NOP receptors of the 1-phenyl-1,3,8-triaza-spiro[4.5]decan-4-one analogues were evaluated measuring calcium mobilization in CHO_{hNOP} cells stably expressing the $G\alpha_{qi5}$ chimeric protein that forces the NOP receptor to couple to calcium signaling. This assay has been previously validated by studying the effects of a large series of NOP receptor ligands encompassing full and partial agonist as well as antagonist activities (30). The novel compounds have been evaluated as NOP receptor agonists using as standard N/OFQ (Figure 3, left panel). Under

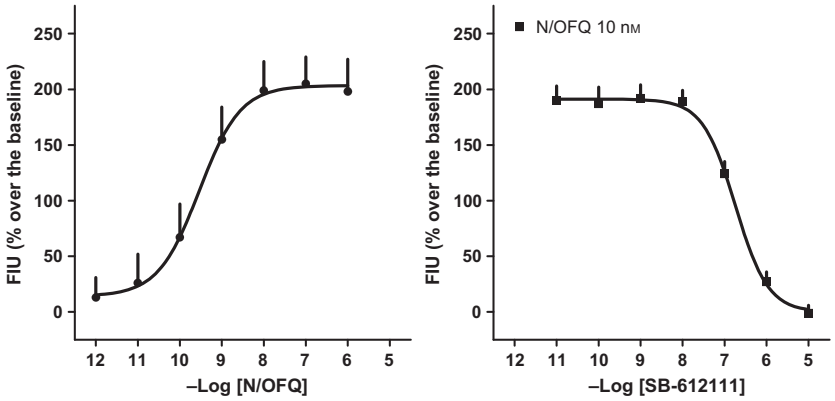

Figure 3: Calcium mobilization experiments performed in CHO cells coexpressing the human NOP receptor and the $G\alpha_{qi5}$ protein. Left panel: concentration response curve to N/OFQ. Right panel: inhibition response curve obtained by challenging 10 nM N/OFQ with increasing concentrations of SB-612111. Data are the mean ± SEM of at least five separate experiments performed in duplicate.

Table 2: Effects of standard and novel NOP ligands in calcium mobilization assays, performed in CHO cells co-expressing the human NOP receptor and the $G\alpha_{qi5}$ protein

Compound		Agonist		Antagonist
		pEC_{50} ($CL_{95\%}$)	$\alpha \pm$ SEM	pK_B ($CL_{95\%}$)
N/OFQ		9.55 (9.07–10.04)	1.00	–
SB-612111		Inactive		8.50 (8.03–8.97)
1	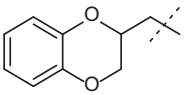	6.49 (5.95–7.03)	0.81 ± 0.03	–
6	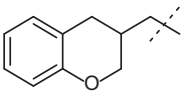	5.97 (5.78–6.17)	1.09 ± 0.05	–
5	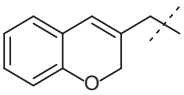	crc incomplete		–
23	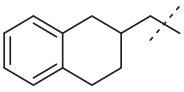	crc incomplete		–
3	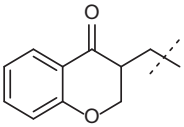	Inactive	Inactive	
17	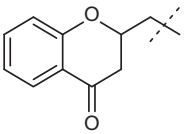	crc incomplete		–
21	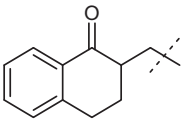	Inactive		<6
***cis*-4**	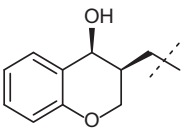	6.67 (6.43–6.91)	0.83 ± 0.04	–
***trans*-4**	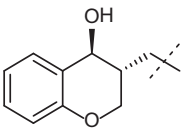	6.45 (5.77–7.13)	0.70 ± 0.02*	–
***cis*-22**	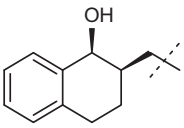	6.38 (5.51–7.25)	1.01 ± 0.41	–

Table 2: continued

Compound		Agonist		Antagonist
		pEC_{50} ($CL_{95\%}$)	$\alpha \pm$ SEM	pK_B ($CL_{95\%}$)
***trans*-22**	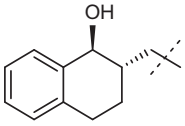	crc incomplete		–
***cis*-18**	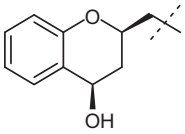	6.57 (6.06–7.08)	1.08 ± 0.32	–
10	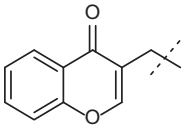	crc incomplete		–
14	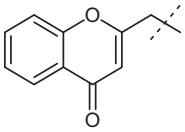	Inactive		<6

Agonist efficacy is expressed as intrinsic activity (α) using the maximal effect elicited by N/OFQ as internal standard ($\alpha = 1.00$).
Inactive: inactive up to 10 μM.
crc incomplete: the concentration–response curve could not be completed because of the low potency of the agonist.
<6: the pK_B could not be precisely determined because the ligand produced a weak inhibitory effect only at the highest concentration tested, that is, 10 μM.
*$p < 0.05$ according to ANOVA followed by the Dunnett test for multiple comparisons.

the present experimental conditions, N/OFQ produced a concentration-dependent stimulation of calcium mobilization with a pEC_{50} of 9.55 and maximal effects of 198 ± 29% over the basal values. These results are close to those previously published (30,31). Results obtained with the novel compounds are summarized in Table 2. Spiroxatrine (**1**), taken as lead compound of this study, behaved as a low-potency NOP agonist with a pEC_{50} of 6.49. Compounds ***cis*-4**, ***cis*-18**, and ***cis*-22** produced a concentration-dependent calcium mobilization with pEC_{50} values of 6.67, 6.57, and 6.38, respectively. The maximal effects elicited by these compounds were not significantly different from that of N/OFQ (Table 2). Compound **6** also behaved as a full agonist showing however lower potency ($pEC_{50} = 5.97$). Compound ***trans*-4** stimulated calcium mobilization in a concentration-dependent manner with a potency value of 6.45. However, the maximal effect induced by this compound was significantly lower than those produced by the standard agonist N/OFQ (Table 2 and Figure 4 panel A). Thus, ***trans*-4** behaved as a partial NOP agonist (Figure 4 panel A). These compounds were inactive up to 10 μM when assayed in CHO cells expressing the $G\alpha_{qi5}$ protein but not the NOP receptor. Thus, the stimulatory effects of compounds **6**, ***trans*-4**, ***cis*-4**, ***cis*-18**, and ***cis*-22** are due to the ability of these molecules to bind and activate the NOP receptor. ***trans*-22** produced an incomplete concentration–response curve at 10 μM, stimulating calcium mobilization to 39 ± 14% over the basal value. Similar results were obtained testing compounds **5**, **10**, **17**, and **23**. Thus, these molecules behaved as low-potency NOP agonists. On the contrary, compounds **3**, **14**, and **21** did not modify calcium levels up to 10 μM. Therefore, these compounds were further evaluated in antagonist-type experiments. In these studies, SB-612111 was used as positive control (30). Inhibition–response curves were performed against a fixed concentration of N/OFQ, approximately corresponding to its EC_{80}. As shown in Figure 3 right panel, under the present experimental conditions, SB-612111 elicited a complete and concentration-dependent inhibition of the N/OFQ stimulatory effect. A pK_B value of 8.50 was derived from these experiments. This value is in line with previously reported findings (21,30). In parallel experiments, compound **3** did not modify the N/OFQ stimulatory effect up to 10 μM. Compound **14** and **21** displayed weak antagonist activity only at the higher concentration tested, that is, 10 μM.

Finally, the selectivity of compounds ***trans*-4** and ***cis*-4** was evaluated measuring calcium mobilization in CHO_{hNOP} cells stably expressing the $G\alpha_{qi5}$ chimeric

protein that forces MOP, DOP, and KOP receptors to couple to calcium signaling. This assay has been previously reported and validated (20). The results obtained are summarized in Table 3 and Figure 4. Compounds ***trans*-4** and ***cis*-4** did not modify calcium levels up to 10 μM in agonist-type experiment for KOP and DOP

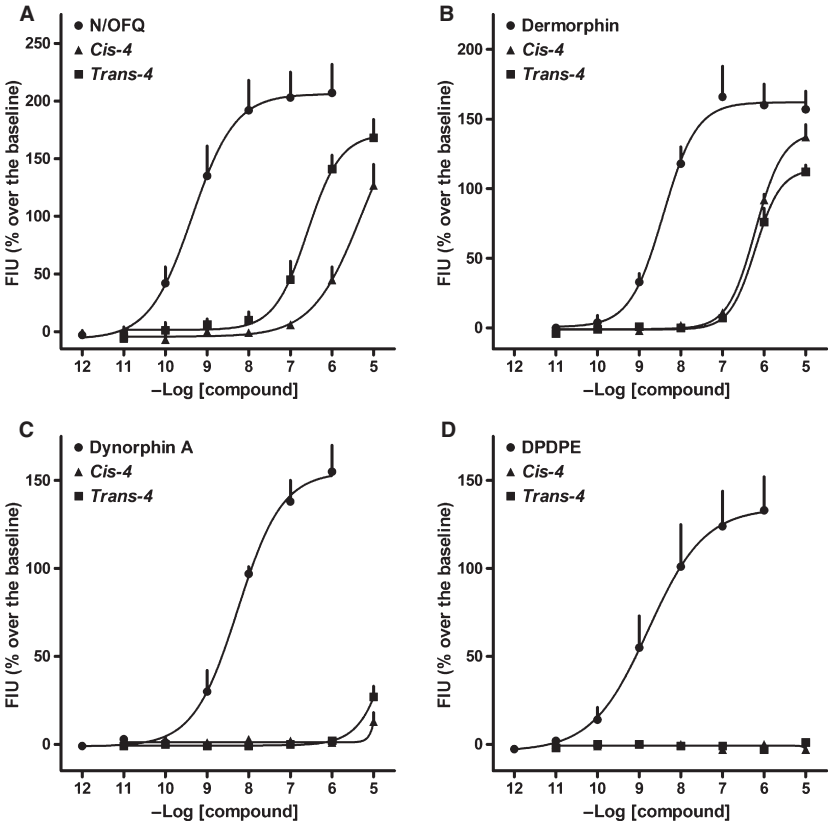

Figure 4: Calcium mobilization experiments performed in CHO cells coexpressing the chimeric G proteins and the human NOP, MOP, KOP, DOP receptors (panels A, B, C, and D, respectively). Concentration response curves to standard agonists, ***cis*-4** and ***trans*-4**. Data are the mean ± SEM of at least three separate experiments performed in duplicate.

Table 3: Effects of ***trans*-4**, ***cis*-4**, and standard NOP, MOP, KOP, and DOP ligands in calcium mobilization experiments performed in CHO cells co-expressing the chimeric G proteins and the human NOP, MOP, KOP, or DOP receptors

	NOP		MOP		KOP		DOP	
	pEC_{50} (CL95%)	α ± SEM	pEC_{50} (CL95%)	α ± SEM	pEC_{50} (CL95%)	α ± SEM	pEC_{50} (CL95%)	α ± SEM
N/OFQ	9.35 (8.86–9.83)	1.00	<5		<6		<5	
Dermorphin	<5		8.43 (7.98–8.87)	1.00	<5		<6	
Dynorphin-A	<6		6.67[a] (6.17–7.17)	0.99 ± 0.05[a]	8.29 (7.45–9.12)	1.00	7.16 (7.07–7.25)	1.10 ± 0.20
DPDPE	Inactive		Inactive		Inactive		8.73 (8.39–9.07)	1.00
***trans*-4**	<6		6.21 (6.00–6.42)	0.87 ± 0.06	Inactive		Inactive	
***cis*-4**	6.68 (5.96–7.41)	0.85 ± 0.08	6.17 (5.88–6.45)	0.73 ± 0.05	Inactive		Inactive	

Agonist efficacy is expressed as intrinsic activity (α) using the maximal effect elicited by N/OFQ as internal standard (α = 1.00).
Inactive: inactive up to 10 μM.
<5 and <6: the concentration–response curve could not be completed because of the low potency of the agonist; the estimated pEC_{50} values obtained by constraining the maximal effects were <5 or 6.
[a]These data were taken from [31].

receptors highlighting a fine NOP/DOP and NOP/KOP selectivity (Figure 4 panel C and D, respectively). Differently, ***trans*-4** and ***cis*-4** produced a concentration-dependent calcium mobilization for the MOP receptor with pEC_{50} values of 6.21 and 6.17, respectively, with a low NOP/MOP selectivity ratio (<0.6 and 3.2, respectively; Table 3). Notably, a reversed behavior in selectivity was observed in comparison with NOP agonist activity, and ***trans*-4** proved to be the most active isomer suggesting complete different stereointeractions with the two NOP/MOP receptors.

Structure–activity relationships of NOP receptor ligands

Isosteric substitution O-1/CH_2 in the 1,4-benzodioxane nucleus of spiroxatrine (**1**), as represented by compound **6**, results in a threefold decrease of agonist potency. A further decrease in potency was observed with the unsaturated benzopyran derivative **5** and with the tetralin derivative **23** with respect to **6**. These results indicate that both oxygen atoms are necessary for spiroxatrine activity at NOP receptors, and the one at position 1 is probably more sensitive to isosteric replacement.

Alternatively, dislocating out of the ring, the oxygen at position 1 and 4 of the 1,4-benzodioxane core of **1** produced the chroman-4-one derivatives **3** and **17**, and it was possible to determine that the introduction of a carbonyl group led to a severe loss of activity. These findings suggest that the introduction of an H-bond acceptor is not well tolerated. In addition, the replacement of oxygen at position 1 of the chroman-4-one derivative **3** provided the inactive α-tetralone derivative **21**, confirming the role of this oxygen. Compounds **3**, **17**, and **21** proved to be inactive also in antagonist-type experiments; these data suggest that these compounds do not bind NOP receptor.

The reduction of carbonyl group of chromanone moiety of **3**, which gave chroman-4-ols ***cis*-** and ***trans*-4**, allowed the recovery of agonist activity, especially in the case of *cis* isomer that showed a pEC_{50} value of 6.67, higher than that of spiroxatrine (6.49). The favorable effect of carbonyl reduction was also observed for compound **22** obtained from the other chromanone derivative **21**. Also in this case, the *cis* isomer was more potent than the *trans* isomer, with a pEC_{50} value of 6.38. Further, confirmation of the positive role of the hydroxyl group in this position came from the comparison of the activities of chromanone **17**, regional isomer of chromanone **3**, and its carbonyl-reduced derivative ***cis*-18** which showed a pEC_{50} value of 6.57. Unfortunately, in the case of this 4-hydroxyl derivative, only the *cis* isomer was obtained. We did not made any further effort to obtain the *trans* isomer as the same isomer of the alcohols **4** and **22** was less active than the *cis* one. For this reason, most likely also in the case of ***trans*-18,** it would have been obtained the same result.

Finally, we wanted to investigate the effect of the introduction of a double bond in the chromanone structure of regional isomers **3** and **17** with the synthesized chromones **10** and **14**. Proceeding from **3** to **10**, a small and barely detectable agonist efficacy was seen, while the contrary seems to be true going from **17** to **14**, as in this case the already weak activity disappears. Certainly, such consideration is based on a very small variation of activity and might be speculative. However, it is suggested that the more constrained structure of these chromones, that makes therefore planar this part of the molecule, does not favor agonist activity. This indirectly seems to confirm the importance first of a certain distortion of the lateral chain and secondly of the oxygenated function in position 4, indicating that the interaction at NOP receptor site is highly stereoselective.

Conclusions

We have synthesized and evaluated several spiroxatrine derivatives as possible NOP receptor ligands. They represent novel tools for better understanding the structural requirements necessary for NOP receptor binding and agonist activity. Moreover, we demonstrated that by introducing specific group on the chromane core of this type of molecules, it is possible to modulate the agonist activity notwithstanding the lipophilic portion is attached to the piperidine nitrogen by a 1-carbon linker. Because the majority of the agonists reported in literature are connected directly to the piperidine nitrogen, this evidence could be useful for the development of new NOP ligands.

Some considerations on structure–activity relationships have led to these conclusions:

1. The presence of an H-bond donator group (hydroxyl group) is more favorable than an H-bond acceptor one (carbonyl group).

2. The H-bond donor group is preferred in α position with respect to the CH_2 linker interposed before the spiropiperidine core.

3. The activities shown by the *hydroxyl derivatives* display a certain degree of stereoselectivity, as *cis* isomers are moderately more active than *trans* isomers.

4. Compound ***cis*-4** shows a promising submicromolar agonistic activity at NOP receptor, and it will be employed as reference compound for the further design and synthesis of other new spiropiperidine-based agonists.

References

1. Meunier J.C., Mollereau C., Toll L., Suaudeau C., Moisand C., Alvinerie P., Butour J., Guillemot J., Ferrara

P., Monsarrat B., Mazarguil H., Vassart G., Parmentier M., Costentin J. (1995) Isolation and structure of the endogenous agonist of opioid receptor-like ORL1 receptor. Nature;377:532–535.
2. Reinscheid R.K., Nothacker H.P., Bourson A., Ardati A., Henningsen R.A., Bunzow J.R., Grandy D.K., Langen H., Monsma F.J., Civelli O. (1995) Orphanin FQ: a neuropeptide that activates an opioidlike G protein-coupled receptor. Science;270:792–794.
3. Zeilhofer H.U., Calò G. (2003) Nociceptin/orphanin FQ and its receptor-potential targets for pain therapy? J Pharmacol Exp Ther;306:423–429.
4. Mika J., Obara I., Przewlocka B. (2011) The role of nociceptin and dynorphin in chronic pain: implications of neuro-glial interaction. Neuropeptides;45:247–261.
5. Mollereau C., Parmentier M., Mailleux P., Butour J.L., Moisand C., Chalon P., Caput D., Vassart G., Meunier J.C. (1994) ORL1, a novel member of the opioid receptor family: cloning, functional expression and localization. FEBS Lett;341:33–38.
6. Calo' G., Guerrini R., Rizzi A., Salvadori S., Regoli D. (2000) Pharmacology of nociceptin and its receptor: a novel therapeutic target. Br J Pharmacol;129:1261–1283.
7. Mogil J.S., Pasternak G.W. (2001) The molecular and behavioral pharmacology of the orphanin FQ/nociceptin peptide and receptor family. Pharmacol Rev;53:381–415.
8. Lambert D.G. (2008) The nociceptin/orphanin FQ receptor: a target with broad therapeutic potential. Nat Rev Drug Disc;7:694–710.
9. Ronzoni S., Peretto I., Giardina G. (2001) Lead generation and lead optimisation approaches in the discovery of selective, non-peptide ORL-1 receptor agonists and antagonists. Exp Opin Ther Patents;11:525–546.
10. Meunier J.C. (1997) Nociceptin/orphanin FQ and the opioid receptor-like ORL1 receptor. Eur J Pharmacol;340:1–15.
11. Meunier J.C. (2000) The potential therapeutic value of nociceptin receptor agonists and antagonists. Exp Opin Ther Patents;10:371–378.
12. Jenck F., Wichmann J., Dautzenberg F.M., Moreau J.L., Ouagazzal A.M., Martin J.R., Lundstrom K., Cesura A.M., Poli S.M., Röver S., Kolczewski S., Adam G., Kilpatrick G. (2000) A synthetic agonist at the orphanin FQ/nociceptin receptor ORL1: anxiolytic profile in the rat. Proc Natl Acad Sci USA;97:4938–4943.
13. Varty G.B., Lu S.X., Morgan C.A., Cohen-Williams M.E., Hodgson R.A., Smith-Torhan A., Zhang H., Fawzi A.B., Graziano M.P., Ho G.D., Matasi J., Tulshian D., Coffin V.L., Carey G.J. (2008) The anxiolytic-like effects of the novel, orally active nociceptin opioid receptor agonist 8-[bis(2-methylphenyl)methyl]-3-phenyl-8-azabicyclo[3.2.1]octan-3-ol (SCH 221510). J Pharmacol Exp Ther;326:672–682.
14. Chiou L.C., Liao Y.Y., Fan P.C., Kuo P.H., Wang C.H., Riemer C., Prinssen E.P. (2007) Nociceptin/orphanin FQ peptide receptors: pharmacology and clinical implications. Curr Drug Targets;8:117–135.
15. Caldwell J.P., Matasi J.J., Zhang H., Fawzi A., Tulshian D.B. (2007) Synthesis and structure-activity relationships of N-substituted spiropiperidines as nociceptin receptor ligands. Bioorg Med Chem Lett;17:2281–2284.
16. Zaveri N., Polgar W.E., Olsen C.M., Kelson A.B., Grundt P., Lewis J.W., Toll L. (2001) Characterization of opiates, neuroleptics, and synthetic analogs at ORL1 and opioid receptors. Eur J Pharmacol;428:29–36.
17. Wichmann J., Adam G., Röver S., Henniq M., Scalone M., Cesura A.M., Daulzenberq F.M., Jenck F. (2000) Synthesis of (1S,3aS)-8-(2,3,3a,4,5,6-hexahydro-1H-phenalen-1-yl)-1-phenyl-1,3,8-triaza-spiro[4.5]decan-4-one, a potent and selective orphanin FQ (OFQ) receptor agonist with anxiolytic-like properties. Eur J Med Chem;35:839–851.
18. Röver S., Adam G., Cesura A.M., Galley G., Jenck F., Monsma F.J., Wichmann J., Dautzenberg F.M. (2000) High-affinity, non-peptide agonists for the ORL1 (orphanin FQ/nociceptin) receptor. J Med Chem;43:1329–1338.
19. Zaveri N., Jiang F., Olsen C.M., Polgar W.E., Toll L. (2005) Small-molecule agonists and antagonists of the opioid receptor-like receptor (ORL1, NOP): ligand-based analysis of structural factors influencing intrinsic activity at NOP. AAPS J;7:E345–E352.
20. Zaratin P.F., Petrone G., Sbacchi M., Garnier M., Fossati C., Petrillo P., Ronzoni S., Giardina G.A., Scheideler M.A. (2004) Modification of nociception and morphine tolerance by the selective opiate receptor-like orphan receptor antagonist (-)-cis-1-methyl-7-[[4-(2,6-dichlorophenyl)piperidin-1-yl]methyl]-6,7,8,9-tetrahydro-5H-benzocyclohepten-5-ol (SB-612111). J Pharmacol Exp Ther;308:454–461.
21. Marti M., Mela F., Budri M., Volta M., Malfacini D., Molinari S., Zaveri N.T., Ronzoni S., Petrillo P., Calo G., Morari M. (2013) Acute and chronic antiparkinsonian effects of the novel nociceptin/orphanin FQ receptor antagonist NiK-21273 in comparison with SB-612111. Br J Pharmacol;168:863–879.
22. Camarda V., Calo' G. (2013) Chimeric G proteins in fluorimetric calcium assays: experience with opioid receptors. Methods Mol Biol;937:293–306.
23. Vogth B.R., Cullison D. United States Patent 1977, 4051248.
24. Sundermann B., Kennies H., Schiene K., Bloms-Funke P., Englberger W., Frormann S., Saunders D. United States Patent 2007, 0203192/A1.
25. Zimmerman D.M., Leander J.D., Cantrell B.E., Reel J.K., Snoddy J., Mendelsohn L.G., Johnson B.G., Mitch C.H. (1993) Structure-activity relationships of trans-3,4-dimethyl-4-(3-hydroxyphenyl)piperidine antagonists for mu- and kappa-opioid receptors. J Med Chem;36:2833–2841.
26. Brady W.T., Agho M.O. (1983) Formation of trans-stilbenes from 1,1-dichloro-2,2-diarylethanes: a new cobaloxime-mediated carbenoid rearrangement. J Org Chem;48:5337–5339.

27. Pearce B.C., Parker R.A., Deason M.E., Dischino D.D., Gillespie E., Qureshi A.A., Volk K., Wright J.J.K. (1994) Inhibitors of cholesterol biosynthesis. 2. Hypocholesterolemic and antioxidant activities of benzopyran and tetrahydronaphthalene analogues of the tocotrienols. J Med Chem;37:526–541.
28. Bolos J., Loscertales T., Nieto J., Sacristàn A., Ortiz J.A. (2000) A new efficient synthesis of 3-(hydroxymethyl)-4H-chromen-4-ones. J Heterocyclic Chem;37:1203–1208.
29. Wipf P., Aslan D.C. (2001) Synthesis of Bicyclic Ortho Esters by Epoxy Ester Rearrangements and Study of Their Ring-Opening Reactions. J Org Chem;66:337–343.
30. Camarda V., Fischetti C., Anzellotti N., Molinari P., Ambrosio C., Kostenis E., Regoli D., Trapella C., Guerrini R., Salvadori S., Calo' G. (2009) Pharmacological profile of NOP receptors coupled with calcium signaling via the chimeric protein Gaqi5. Naunyn Schmiedebergs Arch Pharmacol;379:599–607.
31. Fischetti C., Camarda V., Rizzi A., Pelà M., Trapella C., Guerrini R., McDonald J., Lambert D.G., Salvadori S., Regoli D., Calo' G. (2009) Pharmacological characterization of the nociceptin/orphanin FQ receptor non peptide antagonist Compound 24. Eur J Pharm;614:50–57.

Supporting Information

Additional Supporting Information may be found in the online version of this article:

Appendix S1. Full characterization of compounds **2**–**23**, along with detailed experimental procedures, is given in supplementary file.